X-RAY ABSORPTION SPECTROSCOPY (XAS)

SHELLY D KELLY
Spectroscopy Group Leader
Advanced Photon Source

SPC Group: Yanna Chen, Steve Heald, Juanjuan Huang, Debora Motta Meira, Mike Pape, Aleks Solovyev, George Sterbinsky, Chengjun Sun, Mark Wolfman

July 29, 2024
26th National School on Neutron and X-ray Scattering

OUTLINE

- Background X-ray absorption spectroscopy (XAS)
- X-ray absorption near edge spectra (XANES) process
- XANES examples
- Extended X-ray absorption fine structure (EXAFS) fundamentals
- EXAFS examples

1920 PUBLISHED ABSORPTION EDGES

The K-characteristic absorption frequencies for
The chemical elements magnesium to chromium.
By Hugo Fricke

Synopsis

Absorption of X-rays. –This paper contains an account of an experimental investigation concerning the discontinuity in the x-ray absorption corresponding to the K-series for the chemical elements from magnesium to chromium inclusively. The method followed was the same as that devised and employed by de Broglie. A specially designed vacuum spectrograph was used.

Fine Structure of Absorption. – The spectrograms show that the discontinuity has a rather complex structure, a result in advance of those obtained by earlier investigators. A photometric study of the plates was made in order to obtain a more accurate knowledge of the detailed structure of the absorption limits.

Results. These are recorded in tables which give for each element the wave-lengths of the different remarkable points in the structure of the discontinuities. The theoretical bearing of the new observations is briefly discussed.

https://journals.aps.org/pr/pdf/10.1103/PhysRev.16.202

THE DISCONTINUITY IN THE X-RAY ABSORPTION CORRESPONDING TO THE K-SERIES

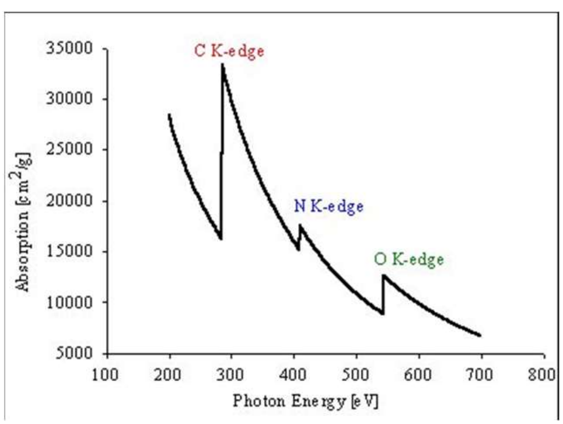

John (https://physics.stackexchange.com/users/101660/john), Why do we have the absorption edge?, URL (version: 2016-02-19): https://physics.stackexchange.com/q/238105

THE DISCONTINUITY HAS A RATHER *COMPLEX STRUCTURE*

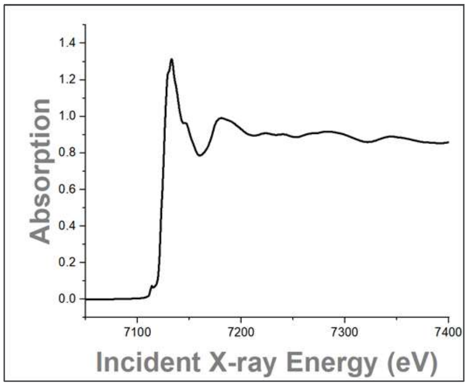

1971 UNDERSTANDING OF EXAFS

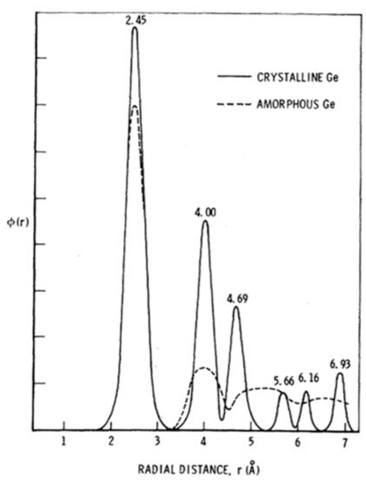

FIG. 2. Fourier transformation of the data of Fig. 1. $\varphi(r)$, a radial structure function, compares amorphous and crystalline Ge. Numbers over the peaks indicate the measured distances in Å.

New Technique for Investigating Noncrystalline structures: Fourier Analysis of the Extended X-ray – Absorption Fine Structure
Dale E. Sayers, Edward A. Stern and Farrel W. Lytle
Physical Review Letters 1971

https://link.aps.org/doi/10.1103/PhysRevLett.27.1204

XANES AND EXAFS

XANES: x-ray absorption near edge structure
EXAFS: Extended x-ray absorption fine structure

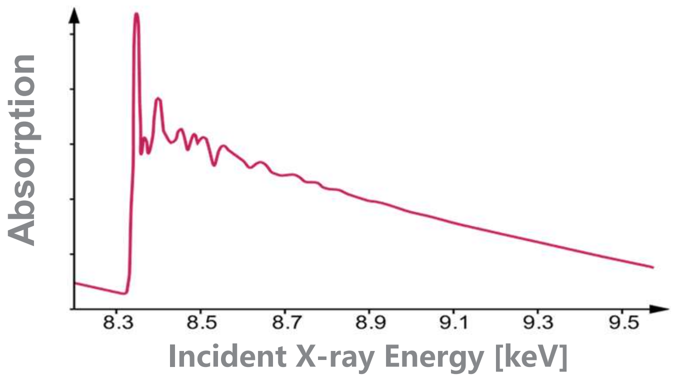

XANES AND EXAFS

XANES: x-ray absorption near edge structure
EXAFS: Extended x-ray absorption fine structure

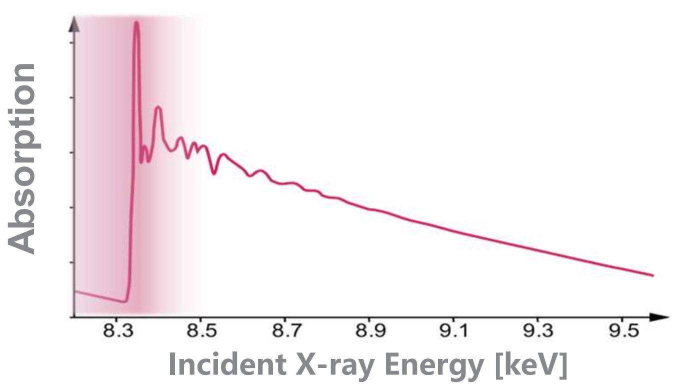

XANES AND EXAFS

XANES: x-ray absorption near edge structure
EXAFS: Extended x-ray absorption fine structure

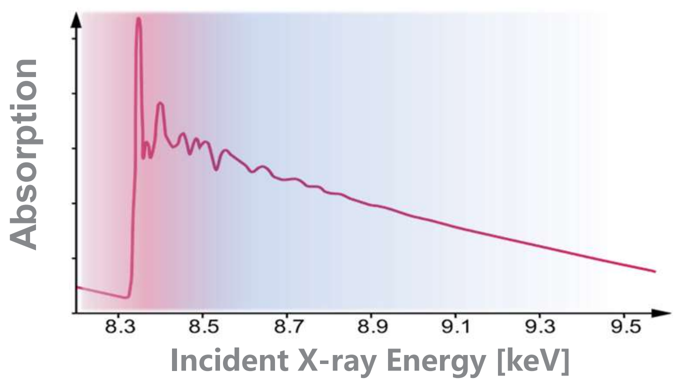

BEER'S LAW: ABSORPTION OF X-RAYS BY MATTER

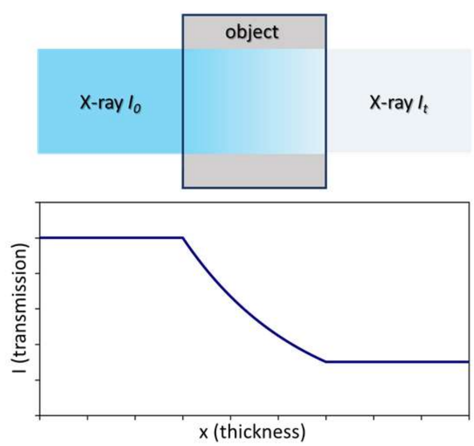

$$I_t = I_0 e^{-\mu x}$$

- μx: absorption length of a material
- One absorption length, I_t = 37% I_0
- Two absorption lengths, I_t = 13% I_0

MEASUREMENT OF X-RAY ABSORPTION COEFFICIENT

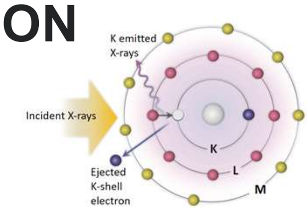

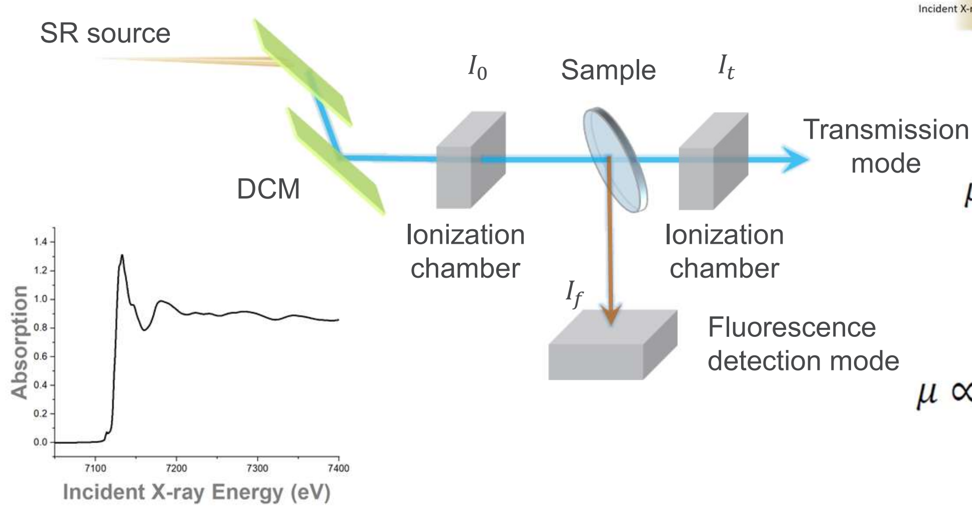

$$\mu = \log \frac{I_0}{I_t}$$

$$\mu \propto \frac{I_f}{I_0}$$

EXPERIMENTAL SETUP AT 25-ID-C

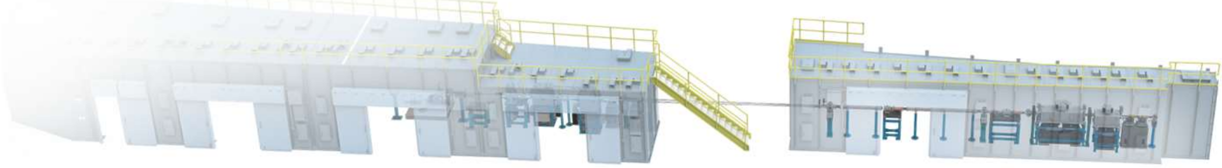

METAL K-EDGE XANES

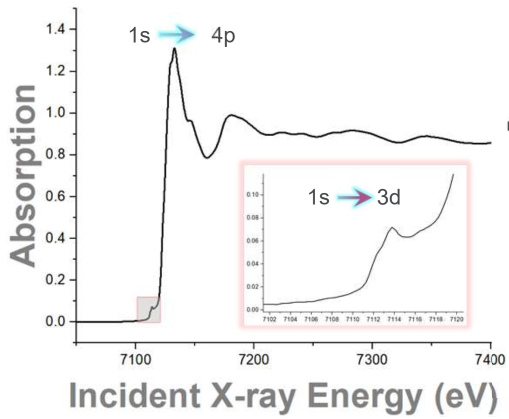

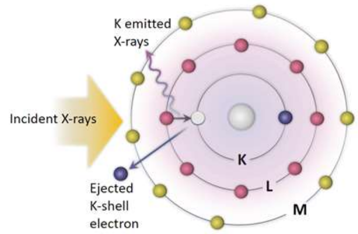

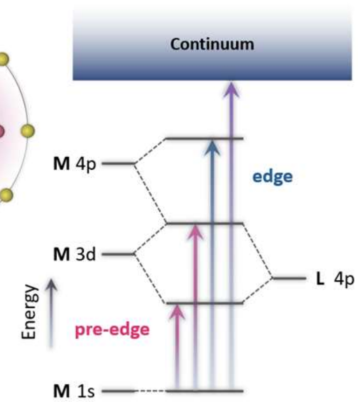

- Absorption edge: dipole 1s → 4p transition ($\Delta l = \pm 1$)
- Pre-edge: mixing of 3d-4p opens 1s → 3d transition

OXIDATION STATE OF MN OXIDES

Mn K-edge XANES

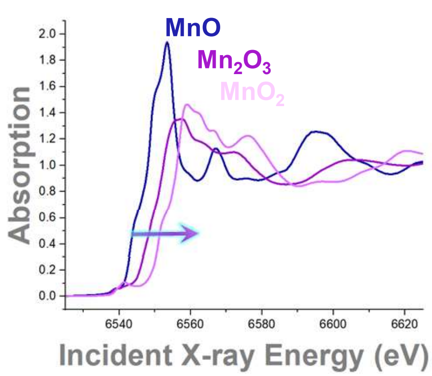

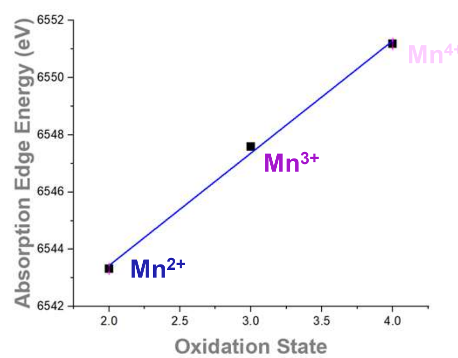

Many elements show significant absorption edge shifts with oxidation state.

PT XANES DURING IN SITU REDUCTION

Direct in situ measurement of Pt reduction

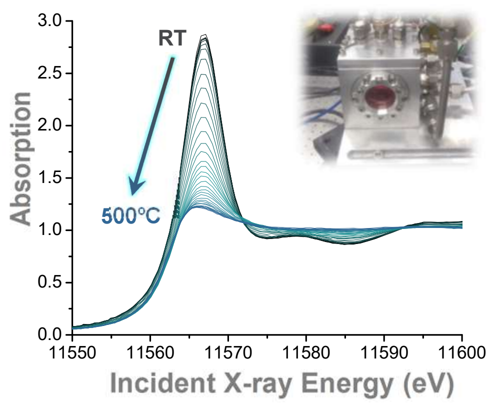

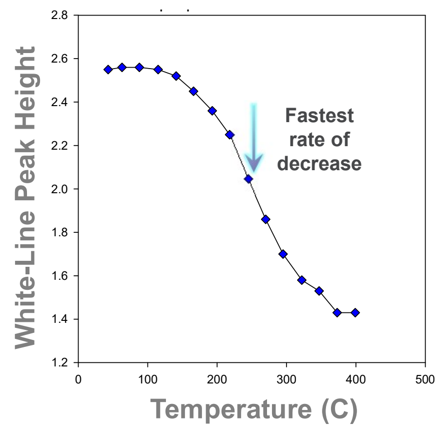

- Pt L_3-edge p->d transition
- Pt electrons: $[Xe]4f^{14}5d^6s^1$
- Pt white line intensity decreases as temperature increases due to 5d electrons filling
- Rate of decrease is fastest at ~270°C.

FAST-CHARGING LITHIUM-ION BATTERIES

Haodong Liu, et al., Nature, 2020

Unique disordered rock salt (DRS) anode reversibly cycles two Li+ at a low 0.6 volts verse a Li/Li+ reference cathode reducing the short-circuit risk due to Li dendrite growth. 40% capacity can be delivered in 20 seconds!

High performance is due to Li intercalation mechanism with low energy barriers and small volume change which cause V to change oxidation state.

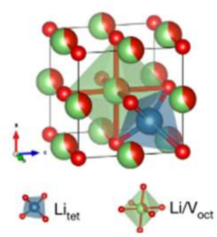

9-BM V K-edge XANES

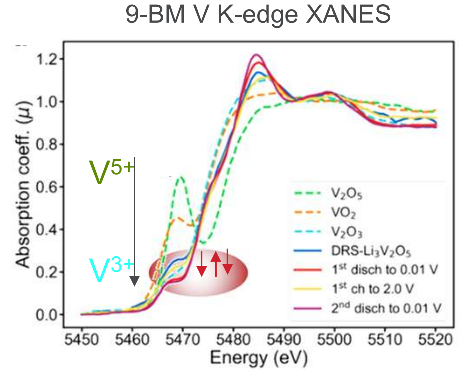

Nudge elastic band calculations

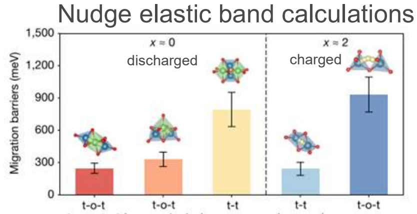

T-O-T Li+ in t-site hops to neighboring occupied o-site, and Li in o-site hops to empty t-site.

T-O-T Li+ in t-site hops through and empty O-site to another t-site

Low energy range at 9-BM enables V K-edge XANES spectra to confirm oxidation state changes with charge and discharge. V in pristine DRS is mixture of V4+ and V3+, after discharge the V oxidation state is less than V3+, oxidation state switches back and forth during the 1st charge and 2nd discharge showing highly reversible V oxidation state change.

The team includes 26 authors with expertise in electrode chemistry, materials synthesis, neutron diffraction, in-situ XRD ICP-OES, STEM, XAS, SEM, XPS, and DFT.

DEFINITION OF EXAFS χ(E)

Normalized oscillatory part of the absorption coefficient

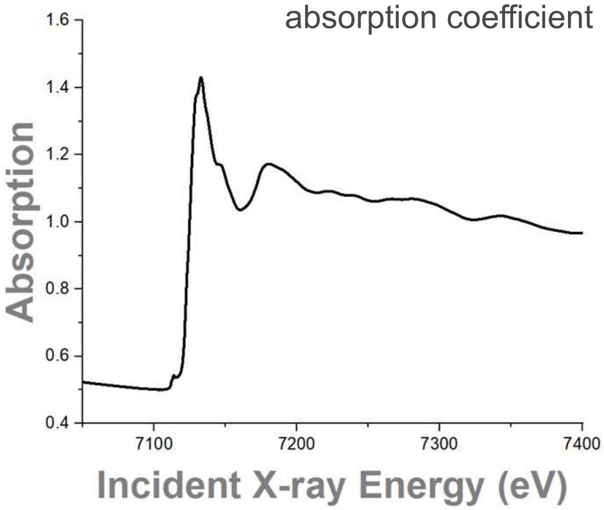

$$\chi(E) = \frac{\mu(E) - \mu_0(E)}{\Delta\mu(E)}$$

Measured absorption coefficient in transmission or fluorescence

$$\mu = \log\frac{I_0}{I_t} \qquad \mu \propto \frac{I_f}{I_0}$$

DEFINITION OF EXAFS: EDGE STEP

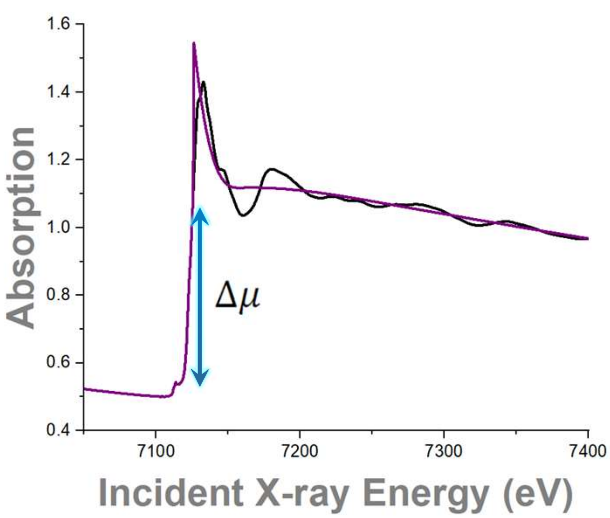

$$\chi(E) = \frac{\mu(E) - \mu_0(E)}{\Delta\mu(E)}$$

Smoothly varying background function, representing the absorption without fine structure

Normalized by the edge step height

DEFINITION OF EXAFS: χ(K)

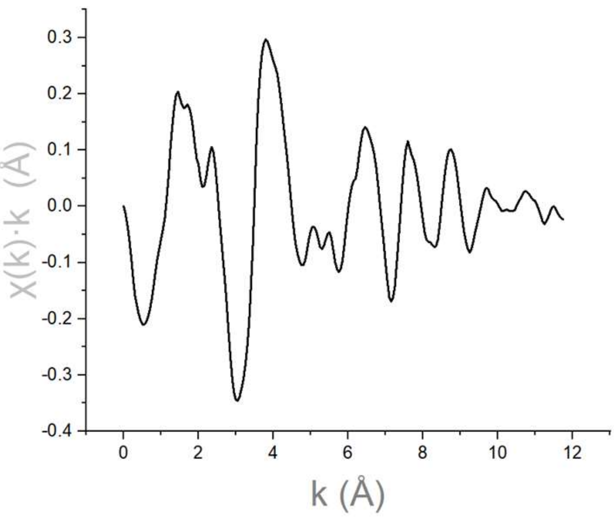

$$\chi(E) = \frac{\mu(E) - \mu_0(E)}{\Delta\mu(E)}$$

$k^2 = 2\, m_e(E\text{-}E_0)/\, \hbar$

FERMI'S GOLDEN RULE

$$\mu(E) \propto |\langle i|H|f\rangle|^2$$

$\langle i|$ Initial State: atom with core electron

H Interaction term: incident x-ray

$|f\rangle$ Final State: atom with core hole, photo-electron

- Transition between two quantum states
- Initial state is well localized at the absorbing atom
- Final state is not, but can be written in terms of two parts

$$|f\rangle = |f_0\rangle + |\Delta f\rangle$$

adsorbing neighboring

X-RAY ABSORPTION FINE STRUCTURE

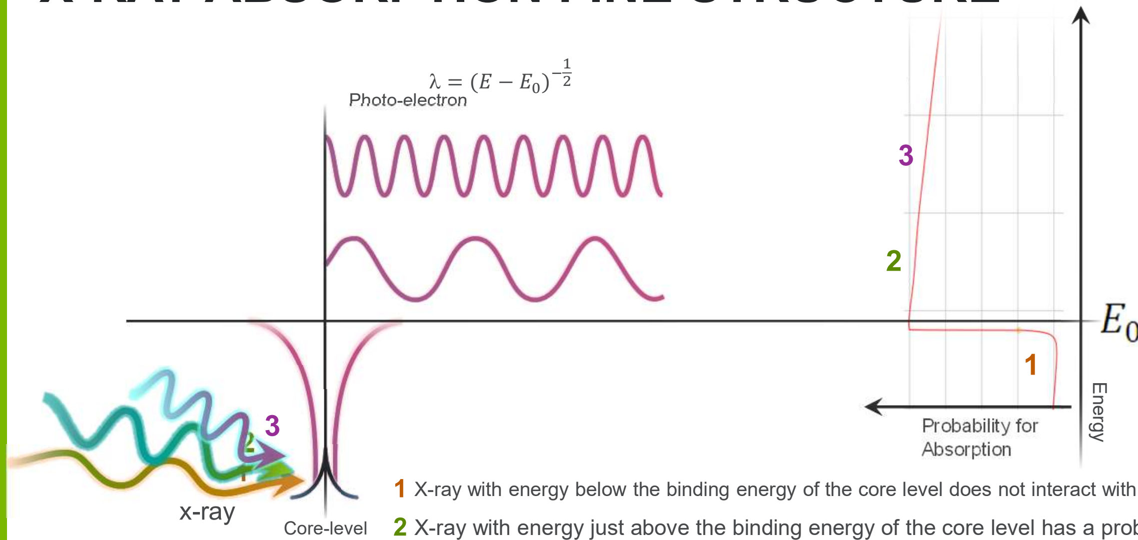

1 X-ray with energy below the binding energy of the core level does not interact with the atom

2 X-ray with energy just above the binding energy of the core level has a probability of being absorbed producing a low energy photo-electron

3 X-ray with higher energy have a probability of being absorbed and producing higher energy photo-electron

X-RAY ABSORPTION FINE STRUCTURE

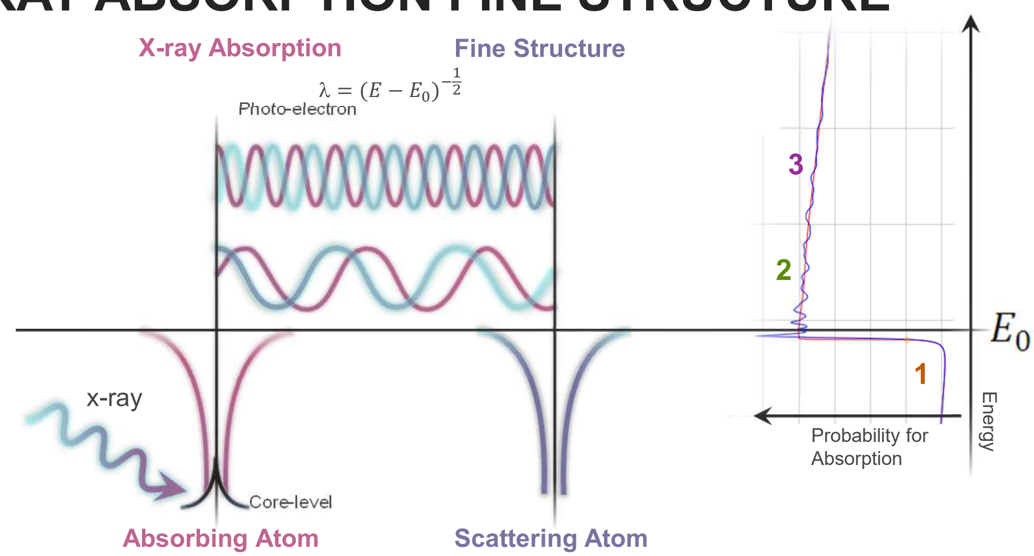

Interference between outgoing and scattered photoelectron at the absorbing atom causes modulations in the probability for absorption.

ADDITIONAL EXAFS DEPENDENCIES

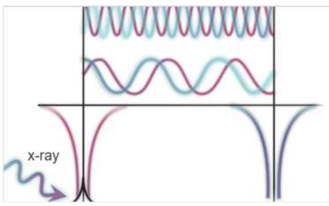

- Atomic Phase shift has two parts. One part from the absorbing atom and another part from the scattering atom.

$$\chi(k) \propto \frac{F(k)}{k^2R^2}\sin(2kR + \delta(k))$$

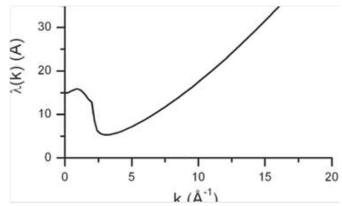

- Mean free path of the photoelectron depends on k causes EXAFS to decrease at high k and contributing to complexity in XANES region at low k

$$e^{-\frac{2R}{\lambda_j}}$$

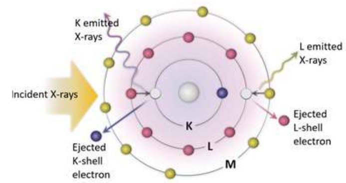

- Passive electron reduction factor: The initial and final states include all the passive electrons of the absorbing atom.

$$S_0^2 = \left|\langle \phi_f^{N-1} | \phi_i^{N-1} \rangle\right|^2$$

AVERAGE OVER SHELLS OF ATOMS

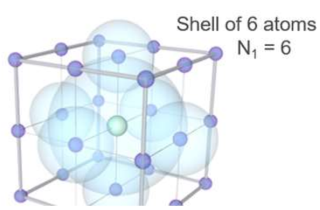

- EXAFS is a sum of all the scattering events of the photoelectron
- Convenient to group "shells of atoms"

$$\chi(k) = \sum_i N_i \chi_i(k)$$

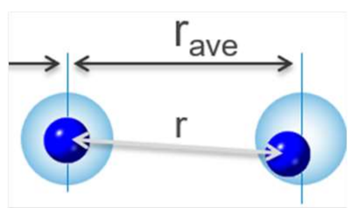

- Not all the atoms in the shell are at the same average distance from the absorbing atom.
- Mean-square displacement of the half path length

$$e^{-2k\sigma^2}$$

THE EXAFS EQUATION

$$\chi(k) = \Sigma_i \chi_i(k)$$

with

$$\chi(k) = \sum_j \frac{N_j S_0^2 F_j(k) e^{-2k^2\sigma_j^2} e^{-\frac{2R}{\lambda}}}{k R_j^2} \sin[2kR_j + \delta_j(k)]$$

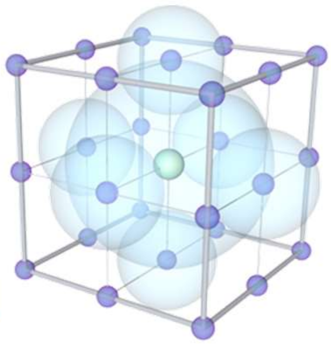

$$R_i = R_0 + \Delta R$$

$$k^2 = 2 m_e(E-E_0)/ \hbar$$

Theoretically calculated values

$F_i(k)$ effective scattering amplitude
$\delta_i(k)$ effective scattering phase shift
$\lambda(k)$ mean free path

Starting values

R_0 initial path length

Parameters determined from a fit to data

N_i degeneracy of path
S_0^2 passive electron reduction factor
σ_i^2 mean squared displacement of half-path length
E_0 energy shift
ΔR change in half-path length

PT EXAFS OF REFERENCE MATERIALS

Pt EXAFS: unique information about the average local atomic environment of Pt

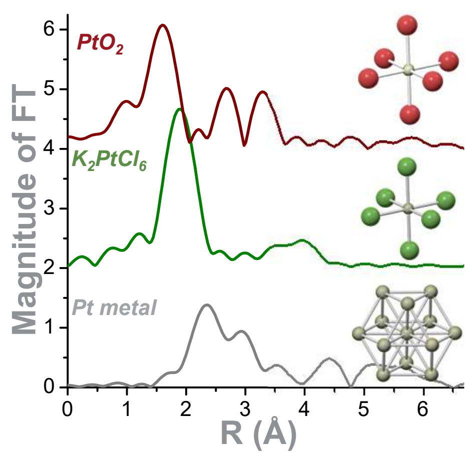

PtO_2		
Neighbor	Number	Distance (Å)
Pt-O	6	2.07
Pt-Pt	6	3.10

K_2PtCl_6		
Neighbor	Number	Distance (Å)
Pt-Cl	6	2.32
Pt-K	4	4.22

Pt metal		
Neighbor	Number	Distance (Å)
Pt-Pt	12	2.77
Pt-Pt	6	3.92

Pt-O, Pt-Cl , and Pt-Pt signals are unique and are readily distinguished.

PLATINUM EXAFS: COMPARISONS WITH FOIL

3 nanometer
959 atoms
Pt-Pt1 CN 10.4

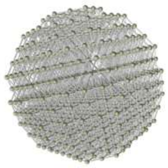

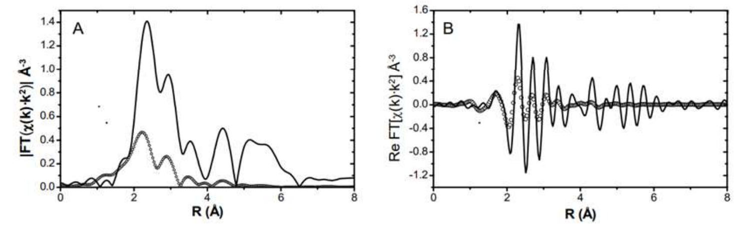

Figure 1. Magnitude (A) and real part of Fourier transform of 300C-reduced (symbols) and Pt foil (solid)

1.0 nanometer
43 atoms
Pt-Pt1 CN 5.4

0.6 nanometer
13 atoms
Pt-Pt1 CN 4.8

6 atoms
Pt-Pt1 CN 4.0

4 atoms
Pt-Pt1 CN 3

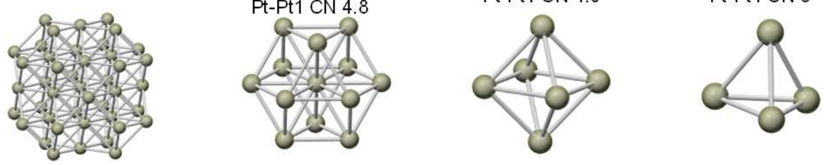

https://iopscience.iop.org/article/10.1088/1742-6596/430/1/012061/pdf

GRAZING INCIDENCE PT EXAFS

Pt monolayer on $SrTiO_3$ (001) substrate

- Oxide supported noble metal nanoparticles are widely used as heterogeneous catalysts; playing an important role for the societal shift from a fossil-fuel to renewable energy sources.
- Studies of highly diluted monolayer and single atom catalyst are difficult, but necessary with catalyst development at the atomic-scale.
- Initial measurements show full EXAFS scans can be used to determine interfacial Pt-O bond

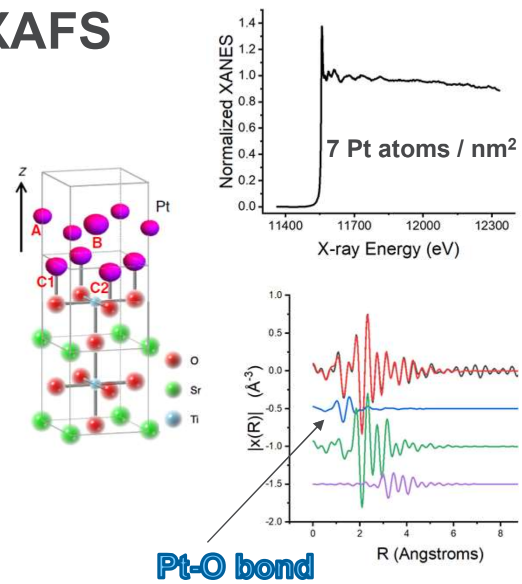

https://doi.org/10.1103/PhysRevLett.128.206801

EXAFS STUDY OF NB_3SN SUPERCONDUCTORS

Heald S. et al., Scientific Reports 2018; Tarantini C, et al. Superconductor Science and Technology 2019

Challenge

- Nb_3Sn proposed for future accelerator upgrades, but needs improved properties
- Doping can offer improvement, but optimization needs better understanding

EXAFS

- Determine dopant lattice location.
- When combined with other results offered key insights into the role of dopants

Result

- Ti, Ta, and Hf dopants studied
- Determined Ta dopant increased antisite disorder with beneficial results
- Hf formed HfO_2 nanoparticle pinning sites
- Combined Ta and Hf doping offers promising route to meeting the needs of future accelerators.

Microprobe needed to measure narrow Nb_3Sn regions

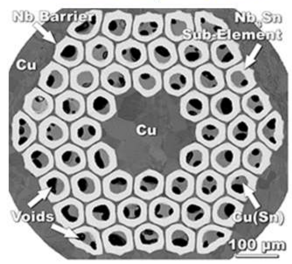

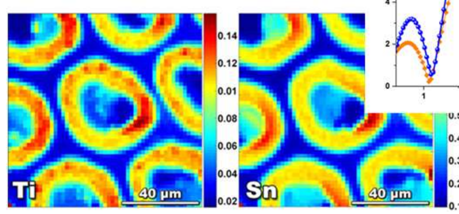

Fourier Transformed EXAFS

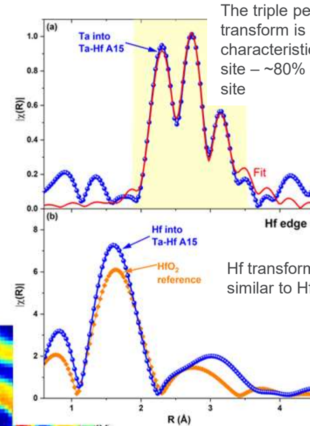

The triple peaked transform is characteristic of the Nb site – ~80% of Ta in Nb site

Hf transform very similar to HfO_2

BONANZA GOLD MECHANISM

Microprobe XRF and Spectroscopy

Extremely high-resolution SR-µXRF mapping of arsenian pyrite reveals that bonanza-style gold mineralization was caused by gold flocculation from electron transfer near arsenic-rich bands.

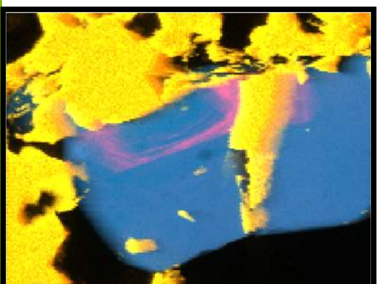

500 µm x 500 µm (50,451 pixels)

As K · Fe K · Au L · Ag K

Colour - Colours scaled independently

The distribution of electrum (Au, ■ + Ag, ■) on the edges of corroded pyrite grains (Fe, ■) with As banding (As, ■) as fine as <2 µm (single pixel thickness!)

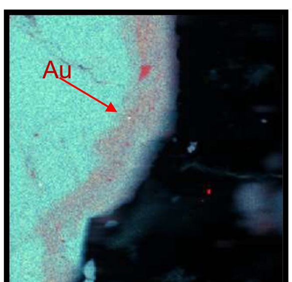

400 µm x 400 µm (40,401 pixels)

Microscopic metallic gold grain (2 pixels wide, ■) within the As band (As, ■) on the edge of a pyrite grain (Fe, ■).

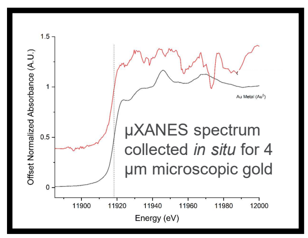

µXANES spectrum collected *in situ* for 4 µm microscopic gold

Microscopic gold within arsenian pyrite growth zone is metallic Au^0 and not lattice bound Au^{+1}

Dr. Neil R. Banerjee, P.Geo.
Dr. Lisa L. Van Loon, C.Chem.

XRF data analysis in Peakaboo (https://peakaboo.org)
Beam spot size: <2 µm x <2 µm
Energy: 26 keV

HIGH TEMPERATURE SHOCKWAVE STABILIZED SINGLE-ATOM CATALYSTS

Yao, et al., Nature Nanotechnology, 2019

Novel general manufacturing route for single-atom catalysts. Shockwaves with controlled 1,500K high-temp and 55ms short on-state followed by longer off-state. Process ensures dispersion and anchoring of metal atoms on substrate defect sites that are highly stable. Overcoming conventional catalyst deactivation mechanism through metal atom agglomeration.

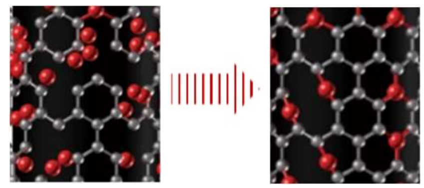

9-BM Pt and Co EXAFS

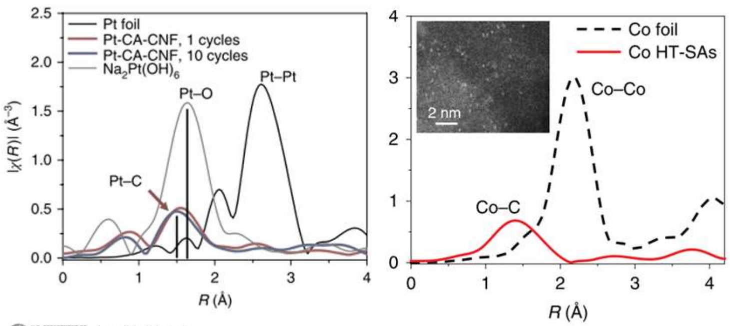

Pt and Co EXAFS at 9-BM shows the typical Metal-C signal that is unchanged from the 1-cycle to the 10-cycle. There is no evidence of agglomeration which would present itself as a strong signal as shown at 2.5 A for metallic foil

The team includes 20 authors with expertise in shockwave materials synthesis, S/TEM, In situ ETEM, Raman spectroscopy, surface area measurements, ICP-MS, EXAFS, MD and DFT simulations, as well as catalysis performance measurements. Tianpin Wu from 9-BM is corresponding author.

https://doi.org/10.1038/s41565-019-0518-7

STRUCTURE OF LUMINESCENT PROTEIN-STABILIZED GOLD CLUSTERS

EXAFS with DFT interpretation


Chemical Science

ROYAL SOCIETY OF CHEMISTRY

EDGE ARTICLE — View Article Online | View Journal | View Issue

Check for updates

Cite this: Chem. Sci., 2018, 9, 2782

Structure and formation of highly luminescent protein-stabilized gold clusters†

D. M. Chevrier,[a] V. D. Thanthirige,[‡b] Z. Luo,[‡c] S. Driscoll,[‡a] P. Cho,[a] M. A. MacDonald,[a] Q. Yao,[c] R. Guda,[b] J. Xie,[c] E. R. Johnson,[a] A. Chatt,[a] N. Zheng[d] and P. Zhang[*a]

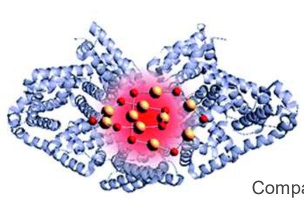

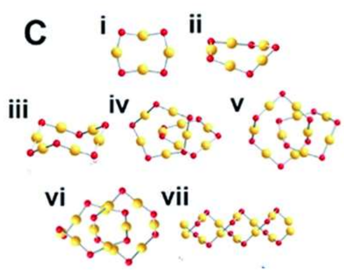

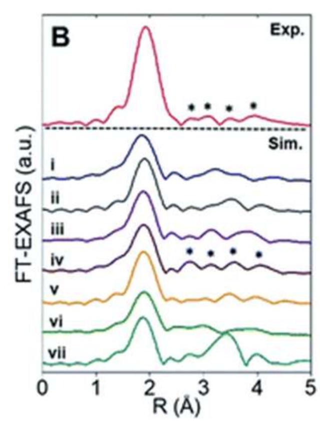

Comparison between DFT simulated structure and measured spectra give insights into the gold cluster morphology

https://doi.org/10.1039/C7SC05086K

Application: XAS on Pd MOF materials

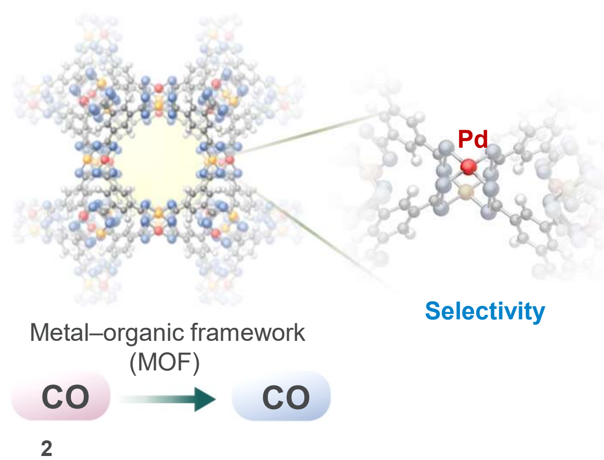

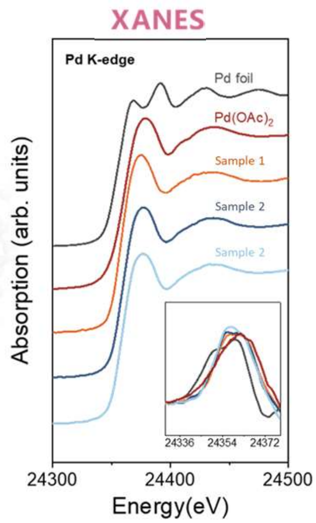

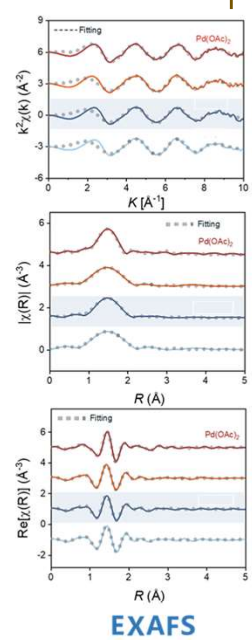

Collaborated with Chair of Inorganic and Organometallic Chemistry, Technical University of Munich

R. Zhang et al. Engineering a Cu-Pd Paddle-Wheel Metal−Organic Framework for Selective CO_2 Electroreduction. *Ready for Submission* ., **2024**

Application: XAS on Pd MOF materials

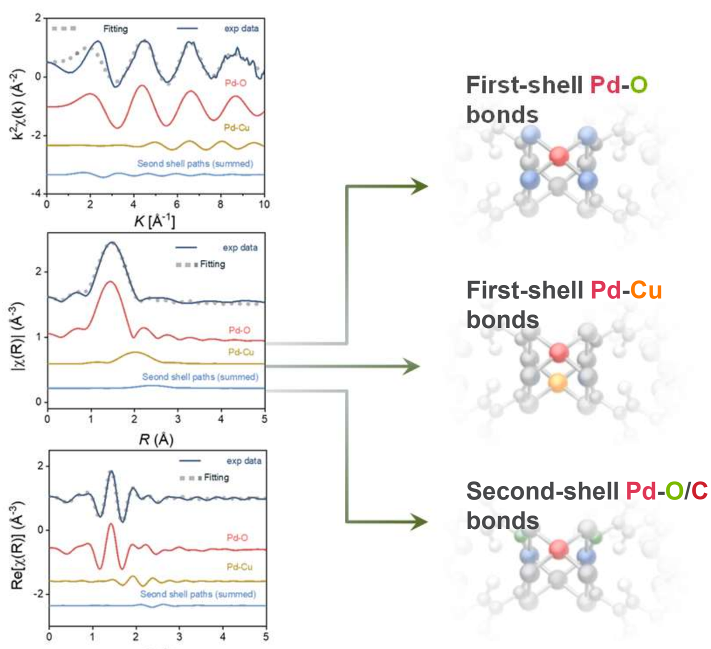

Scattering Path	N_{coor}	R [Å]
Pd-O	4	1.98 ± 0.01
Pd-Cu	1.05 ± 0.56	2.50 ± 0.01
Pd-C	4	2.81 ± 0.02
Pd-O-C	8	3.03 ± 0.02
Pd-O	4	3.05 ± 0.02

Our model verifies the validation of Pd-Cu paddle-wheel structure

R. Zhang et al. *Ready for submission* ., **2024**

Q & A

Kelly, S. D.; Hesterberg, D.; Ravel, B.; Analysis of Soils and Minerals Using X-Ray Absorption Spectroscopy. Methods soil Anal. Part 5. Mineral. methods 2008, 5, 387–464.